Petroleum Research

Petroleum Research 2019(October-November), Vol. 29, No. 107, 36-39

DOI: 10.22078/pr.2019.3468.2585

Improving the Photocatalytic Performance of $BiFeO_3$ Perovskite for Overall Water Splitting Reaction

Hadis Sepahvand and Sharam Sarifnia*

Catalyst Research Center, Chemical Engineering Department, Razi University, Kermanshah, Iran

sharif@razi.ac.ir

DOI: 10.22078/pr.2019.3468.2585

Received: September/15/2018 Accepted: May/22/2019

INTRODUCTION

One of the major challenges of the twenty first century is keeping up with the growth in global energy demand due to increasing population and rising standards of living. For instance, in 2011, 15 TW-energy was consumed by approximately seven billion people world-wide. By 2050, these numbers are expected to escalate to 30 TW and nine billion people respectively [1].

Hydrogen can be the best alternatives to fossil fuels owing to its obvious advantages. Hydrogen generation by overall water splitting using a suitable semiconductor photocatalyst provides an efficient strategy to achieve the clean and sustainable energy [2]. Thermodynamically, water decomposition into oxygen and hydrogen is a non-spontaneous reaction (change in Gibbs free energy> 273 kJ/mol) with an uphill nature, and in the past decades, extensive attempts have been made to find beneficial photocatalysts for this reaction [3,4]. $BiFeO_3$ as a ferroelectromagnetic perovskite with optical band gap of ~2.3 eV has significant potential for the photo-induced water oxidation [5].

In this work, the improved heterojunction of $BiFeO_3$ were synthesized by a facile and cost-effective method, for hydrogen generation through photocatalytic overall water splittin.

EXPERIMENTAL PROCEDURE

CATALYST PREPARATION

In a typical synthesis process, the equimolar ratio of $Fe(NO_3)_3$.9H2O (1.010 g) and $Bi(NO_3)_3.5H_2O$ (1.213 g) were mixed and dissolved in 10 mL dilute nitric acid. Subsequently, 30 mL KOH (8.0 mol/L) solution as mineralizer was poured drop-wise to the resulting transparent solution. Next, the brown suspension was vigorously stirred for 30 min at room temperature to be uniform completely. The resulting was transferred

into 50 mL Teflon-lined stainless autoclave. The hydrothermal treatment was performed at 200 °C for 6 h. For g-C_3N_4 synthesis, 3 g of melamine by an alumina crucible possess a proper cap was put into a muffle furnace and heated to 550 °C for 4 h with a heating rate of 5 °C/min.

For prepare ZnS first, 10 mL of 0.5M zinc acetate dehydrate solution (Zn $(OAC)_2 \cdot 2H_2O$) along with 10mL of 0.5M sodium sulfide solution (Na2S·$9H_2O$) were stirred on a stirrer. Then these two, in drops, were added into 10 mL of 0.5M sodium dodecyl sulfate (SDS), and the solution was placed on a stirrer for 30 min to obtain a homogeneous solution. The obtained solution was then passed through a filter paper. Finally, the obtained precipitates were placed in the oven at 60 °C for 24 h.

For preparation of $BiFeO_3$/g-C_3N_4 composite appropriate amounts of as-prepared g-C_3N_4 and $BiFeO_3$ powder were mixed and crushed together and then calcinated via a muffle furnace at 300 °C pending 1 h. To prepare the couple of $BiFeO_3$/ZnS at the end of ZnS synthesis, the $BiFeO_3$ powder was added to the solution and placed under ultrasonic for 30 min. Then, it was filtered and the obtained precipitates were dried at 80 °C for 24 h.

CATALYTIC ACTIVITY TEST

Water splitting reactions were performed in a 160 mL self-designed photoreactor irradiated by three 125 W medium pressure Hg lamps as UV source. 0.04 g of photocatalyst sample was dispersed in 100 mL water without using any sacrificial agent under magnetic stirring. The hydrogen production was determined by gas chromatography (GC), equipped with a thermal conductivity detector (TCD) and a Molecular Sieve 5 $\mathring{A}$ column.

RESULTS AND DISCUSSION

CHARACTERIZATION

The XRD are illustrated in Fig. 1. It is apparent that the perovskite structure of BFO with high purity was well crystallized (JCPDS Card No. 14-0181). Characteristic peaks of g-C_3N_4 located at 13.2 and 27.5° represent (100) and (002) diffraction planes for graphitic materials respectively (JCPDS Card No. 87-1526). The XRD pattern of ZnS has a number of diffraction peaks in 2θ=57.52°, 48.94°, and 30.16° which were, respectively, related to (311), (220), and (111) faces of the hexagonal crystalline structure of ZnS Wurtzite. The XRD pattern of composite shows the diffraction peaks of both of elements, demonstrating the coexistence of elements in the composite sample.

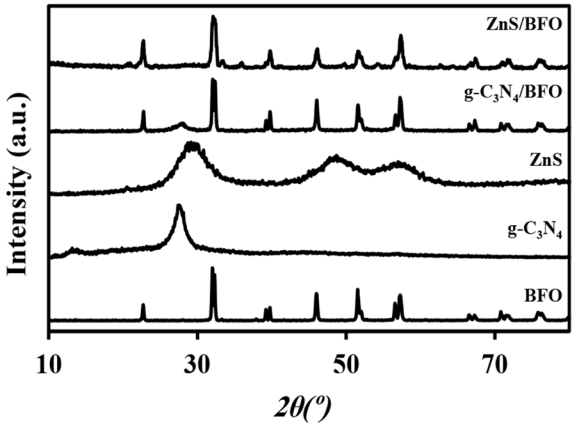

Figure 1: XRD patterns of synthesized samples.

As shown in Fig. 2, the highest intensity of PL signal relates to ZnS and indicates the fast recombination due to its nature. Although BFO has a limited band gap, but its multiferroic properties and self-polarization cause extending the lifetime of the photoexcited charges considerably. In the composites, the lower recombination rate is a result of electric field formation in the p-n heterojunction. Also, closely contacted interfaces between photocatalysts promote the electron-hole separation efficiency.

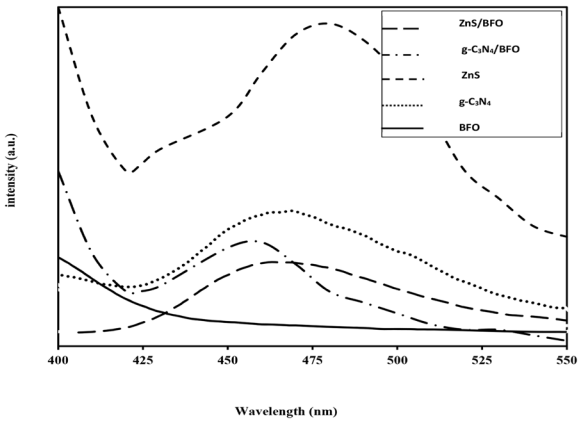

Figure 2: PL spectra of synthesized samples.

CATALYTIC PERFORMANCES

The photocatalytic gas productions toward water splitting over different samples are illustrated in Fig. 3. The pure BFO and ZnS did not show any activity for overall water splitting, which could be ascribed to the inappropriate band position and low energy level of the photoexcited electron-hole pairs. Furthermore, pure g-C_3N_4 showed insignificant gas production ability under UV light irradiation caused by the fast recombination rate. In contrast, composite samples exhibited favorable activity in hydrogen production. The rate of hydrogen production by BFO/ZnS and BFO/g-C_3N_4 are ~ 44.75 and 160.75 µmol h^{-1} g^{-1}, respectively.

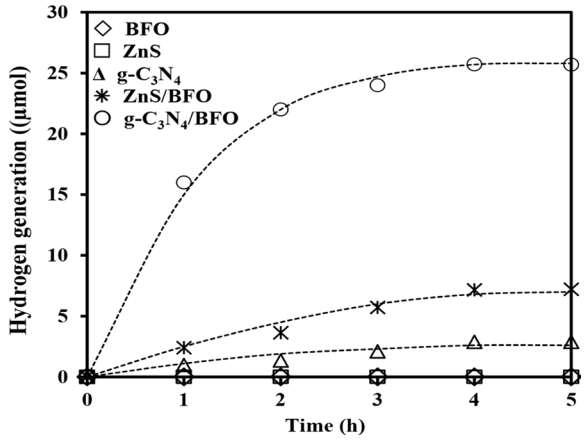

Figure 3: Time-profiled gas production of synthesized photocatalysts.

CONCLUSIONS

The pure BFO despite its unique features, such as the low rate of electron-hole recombination, it is not capable of producing hydrogen during the overall water splitting reaction. Also, ZnS is virtually inactive in the overall water splitting reaction. The rate of hydrogen production by pure g-C_3N_4 is 18 µmol h^{-1} g^{-1}. In contrast, composite samples exhibited favorable activity in hydrogen production. The rate of hydrogen production by BFO/ZnS and BFO/g-C_3N_4 are about 44.75 and 160.75 µmol h^{-1} g^{-1}, respectively. The enhanced overall water splitting performance is attributed to the synergetic effect advantages and effective separation of electron-hole pairs. Finally, these results revealed the effective utilization of junction architecture for hydrogen production.

REFERENCES

[1]. Dincer I. and Acar C., *"Review and evaluation of hydrogen production methods for better sustainability,"* International journal of hydrogen energy., Vol. 40, No. 34, pp. 11094-11111, 2015.

[3]. Tee S. Y., Win K. Y., Teo W. S., Koh L. D., Liu S., Teng C. P. and Han M. Y., *"Recent Progress in Energy-Driven Water Splitting,"* Advanced Science., Vol. 4, No. 5, p. 1600337, 2017.

[4]. Hisatomi T., Kubota J. and Domen K., *"Recent advances in semiconductors for photocatalytic and photoelectrochemical water splitting,"* Chemical Society Reviews., Vol. 43, No. 22, pp. 7520-7535, 2014.

[5]. Kong D., Zheng Y., Kobielusz M., Wang Y., Bai Z., Macyk W. and Tang J., *"Recent advances in visible light-driven water oxidation and reduction in suspension systems,"* Materials Today., Vol. 21, No.

8, pp. 897-924, 2018.

[8]. Manzoor A., Afzal A. M., Umair M., Ali A., Rizwan M. and Yaqoob M. Z., *"Synthesis and characterization of Bismuth ferrite ($BiFeO_3$) nanoparticles by solution evaporation method,"* Journal of Magnetism and Magnetic Materials., Vol. 393, pp. 269-272, 2015.